Bollettino di Geofisica Teorica ed Applicata Vol. 61, n. 4, pp. 499-516; December 2020
DOI 10.4430/bgta0321

Determination of surface deformations in Bolvadin Fault by the precision levelling method and investigation of the relationship with underground water

İ. Tiryakioğlu[1,2] and H. Basri Bozkuş[1]

[1] *Department of Geomatics, Faculty of Engineering, Afyon Kocatepe University, Afyonkarahisar, Turkey*

[2] *Earthquake Research and Implementation Center, Afyon Kocatepe University, Afyonkarahisar, Turkey*

(Received: 20 November 2019; accepted: 17 January 2020)

ABSTRACT In this study, the amount of aseismic surface deformation occurring in the centre of the Bolvadin district in the last 10 years was determined by the precision levelling method. Bolvadin district centre has a levelling network consisting of eight profiles perpendicular to the surface deformations, and 12 levelling measurement campaigns were undertaken from 2016 to 2018. From the measurements, it was calculated that over two years, the deformations had reached 100 mm in the study area. Subsequently, the data were collected from the 18th Regional Directorate of the State Hydraulic Works on three water wells in the region showing groundwater levels. It was determined that underground water levels had decreased 5 m in 24 months. Kendall, Spearman and Pearson correlation methods were used to investigate the correlation between groundwater levels and deformations. The results revealed that there was a moderate correlation between surface deformations and decrease in ground water levels except for wells 4 and 5.

Key words: precision levelling, Bolvadin Fault, underground water, surface deformation.

1. Introduction

Surveying vertical crustal movements provides an important foundation for the study of earthquakes and seismic surface deformation. In recent years, precise levelling, Global Navigation Satellite System (GNSS), and Interferometric Synthetic Aperture Radar (InSAR) technics have supported geodetic techniques to obtain vertical deformation information of the Earth's surface, with millimetre or even sub-millimetre precision. According to GNSS and InSAR technics, precise levelling is highly accurate, but has obvious disadvantages, such as low efficiency, elevated labour costs, and high transmission errors. In recent years, with the production of digital levelling, many of these disadvantages in the precision levelling technique have disappeared. Therefore, digital level usage has increased, especially in the monitoring of vertical deformations (D'Anastasio *et al*., 2006; Murasea *et al*., 2013; Hao *et al*., 2014; Kall *et al*., 2014; Sabuncu and Ozener, 2014; Amighpey and Arabi, 2016; Qin *et al*., 2018; Poyraz *et al*., 2019; Tiryakioğlu *et al*., 2019).

Seismic surface deformations are classified as surface faults and Earth fissures (Holzer, 1984; Péwé, 1990; Holzer and Galloway, 2005; Pacheco-Martínez *et al*., 2013; Özkaymak *et al*., 2017). Earth fissures forming straight to arcuate patterns are caused by stretching related to the bending of strata above a localised differentially compacting zone. Fissures forming complex polygonal patterns are probably caused by tension induced by capillary stresses in the zone above a declining water table. Surface faults occur along pre-existing faults, many of which behave as partial groundwater barriers (Holzer, 1980, 1984). Vertical displacement is observed in the surface faults, and deformations continue towards the deeper points. However, the vertical displacements are not observed through the surface fractures; the expansions perpendicular to the fractures are seen, and those fractures were absorbed in depths close to the surface and not much deeper.

In Turkey, western Anatolia is one of the most important seismogenic zones having a major tectonic structure consisting of the Fethiye - Burdur Fault Zone (FBFZ), Isparta Angle (IA), Gediz Graben, and Akşehir - Sultandagi Fault Zone (ASFZ) (Fig. 1a). In recent years, seismic surface deformations have been observed along the active margin faults of grabens in western Anatolia. One of the surface deformations (Tiryakioğlu *et al*., 2018a, 2018b, 2019; Özkaymak *et al*., 2019) is located on the Bolvadin Fault (Fig. 1) in the Afyon Akşehir Graben (AAG) that represents the south-eastern part of Akşehir - Simav Fault System (ASFS).

The reasons for these surface deformations have been discussed in various studies. Based on InSAR images, İmamoğlu *et al*. (2019) contended that those deformations were derived completely from a decrease in underground water. However, Özkaymak *et al*. (2019) and Tiryakioğlu *et al*. (2019) argued that those deformations might be tectonic based together with underground water.

In this study, 12 precise levelling surveys were conducted to determine the amounts of the surface deformations occurring in the Bolvadin settlement located in the middle of AAG. The data were obtained from the water observation well in the region to determine the underground water level. Whether the underground water displacement is related to those deformations is determined by the Pearson, Spearman-Rank, and Kendall-Tau functions. There was a statistically moderate relationship between underground water levels and deformations.

2. Tectonic settings

AAG is an approximately 130 km long, 4 to 20 km wide, NW-SE-trending, actively growing continental rift zone. The zone represents the border of central Anatolia to the north and the IA to the south (Blumenthal, 1963; Koçyiğit, 1984; Koçyiğit *et al*., 2000; Koçyiğit and Özacar, 2003; Tiryakioğlu, 2018a; Özkaymak *et al*., 2019). The south-eastern border of the middle part of AAG is controlled by the Sultandağı Fault (SF), a 90 km long active dip-slip normal fault responsible for the 2002 Çay earthquakes (M_W 6.3 and 6.0). These faults cause most of the earthquakes recorded in both historical and instrumental earthquake catalogues in the region. Addition to the SF, the northern border faults of the middle part of AAG are *en échelon* NE-SW trending dip-slip normal faults, namely the Bolvadin Fault (BF), Büyük Karabağ Fault (BKF), and Çukurcak Fault (ÇF) (Özkaymak *et al*., 2017, 2019; Tiryakioğlu *et al*., 2018a). Geologic mapping studies on the BF indicate that it typically has a NE-SW-striking and SE dipping sense extending approximately 16 km between Bolvadin settlement to the SW with an approximately wide of 2 km (Fig. 1a). Extensive knowledge concerning the BF and the earthquakes it produces can be obtained from

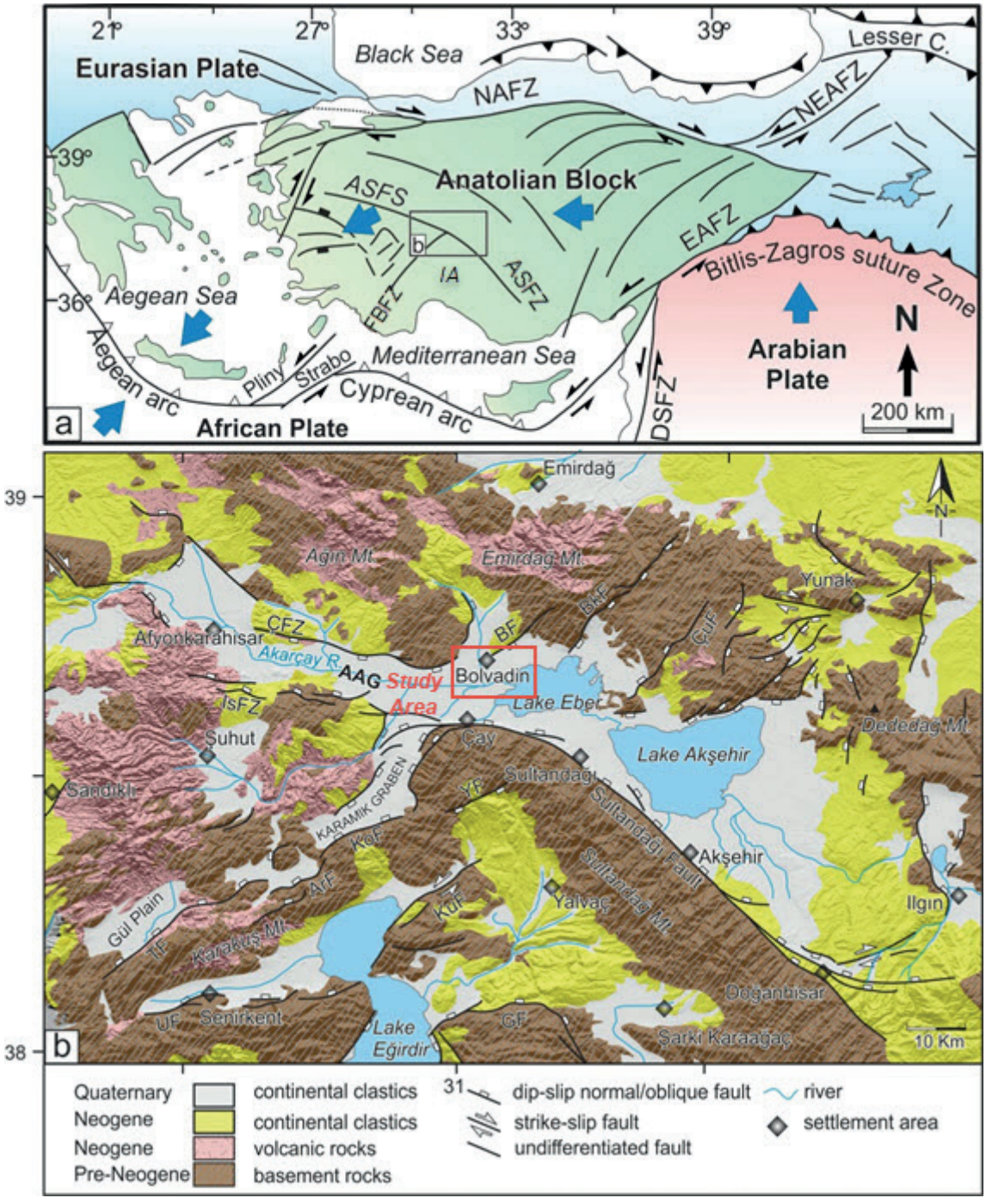

Fig. 1 - a) Tectonic outline of the eastern Mediterranean area [compiled from Kaymakci (2006) and Özkaymak (2015)]. Abbreviations: ASFS: Akşehir - Simav Fault System; DSFZ: Dead Sea Fault Zone; EAFZ: East Anatolian Fault Zone; NAFZ: North Anatolian Fault Zone; NEAFZ: NE Anatolian Fault Zone. b) Geology map of AAG and immediate vicinity [compiled from Turan (2002), Emre *et al*. (2011) and Özkaymak *et al*. (2017)]. Abbreviations: ÇFZ: Çobanlar Fault Zone; IsFZ: Işiklar Fault Zone; BF: Bolvadin Fault; BkF: Büyük Karabağ Fault; ÇuF: Çukurcak Fault; YF: Yarikkaya Fault; KuF: Kumdanlı Fault; GF: Gelendost Fault; KoF: Kocbeyli Fault; ArF: Arızli Fault; UF: Uluborlu Fault; TF: Tatarli Fault (Tiryakioğlu *et al*., 2019).

the work of Özkaymak *et al*. (2019). Over the last 10 years, some linear surface deformations, from the south-western side of the town to the north-western side, have been observed related to the BF (Fig. 2). During field studies in the Bolvadin area, progressive surface deformations, such as surface faults and Earth fissures, with lengths varying from 300 m to 2 km and strike varying between N15°E and N70°E, were mapped (Özkaymak *et al*., 2017, 2019).

2.1. Determination of surface deformation with precise levelling surveys and underground water levels

Since 2012, deformations previously not observed have formed on the surface of the centre of the Bolvadin settlement, which is generally founded on alluvium soil, and these deformations are continuing to form. In order to determine the amount of vertical surface deformations, a precise

Fig. 2 - Field photographs showing the vertical displacement along surface deformation.

levelling network was established in the region. Surface deformations in the region are visible. Therefore, the profiles are designed as cross-sectional profiles of surface deformations. The network consists of 79 benchmarks (Fig. 3) which were installed on concrete electrical supply poles.

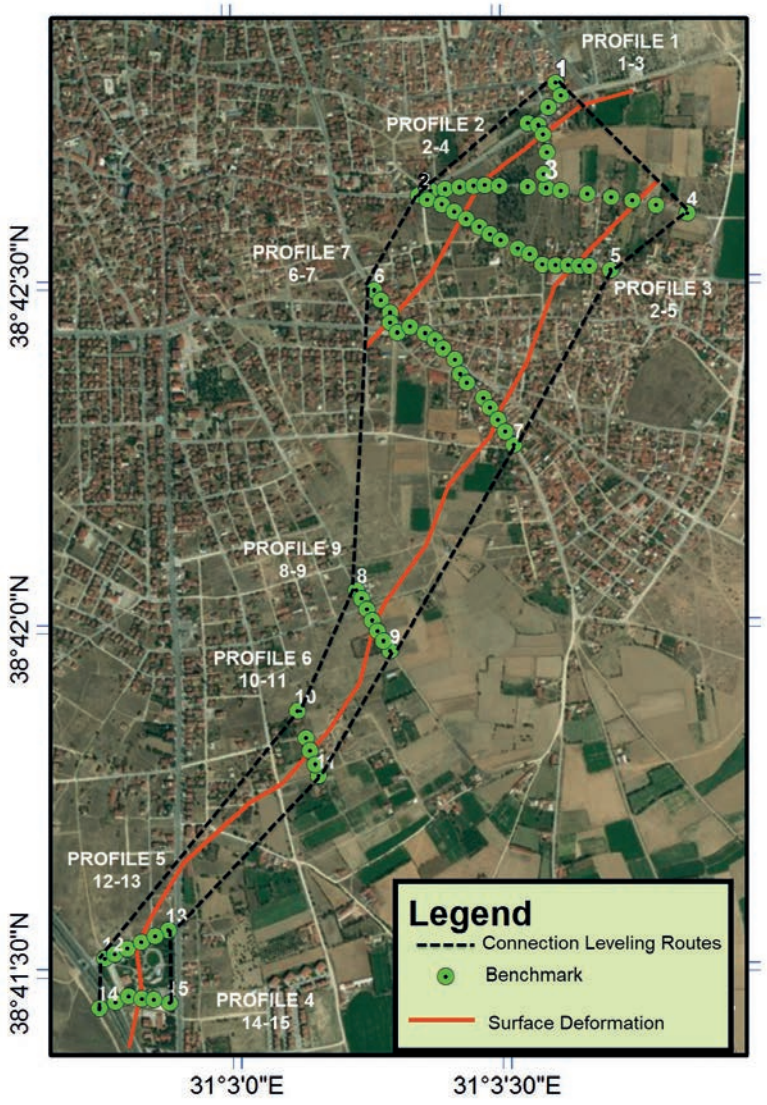

Fig. 3 - Precise levelling network. Red lines show the surface deformations, green circle indicates the levelling profiles and benchmark, the black dot line shows the connection levelling routes.

For all routes, the precise levelling surveys were conducted forwards and backwards using the digital Topcon DL-101C with calibrated and barcoded invar rods. The manufacturer specified the precision of the instrument as ±0.4 mm for a 1 km long, double levelling run with a coded Topcon invar rod (Rüeger, 2000). The Backsight-Foresight-Foresight-Backsight (BFFB) method was used as one of the precision levelling measurement methods (Fig. 4). The invar rods were read three times using digital levels, and this process was repeated when the difference between the readings was greater than 0.4 mm. The differences between the round-trip measurements on

all routes did not exceed the error limit calculated by the $4\sqrt{S_{(km)}}$ formula specified in the German standard (DIN-18710). $S_{(km)}$ represents the length of section in kilometres. Information concerning the established levelling network was taken from Tiryakioğlu *et al*. (2019). The levelling network measurements were made between 2016 and 2018 over 12 campaigns (Table 1). To determine the seasonal behaviour of the deformations occurring in the region, levelling measurements were undertaken in all seasons.

Fig. 4 - Levelling measurements (August 2018).

Table 1 - Dates and period intervals of levelling measurements.

Campaign Number	Dates	Period Interval (Mount)	Campaign Number	Dates	Period Interval (Mount)
1	19.08.2016	0	7	15.11.2017	15
2	07.05.2017	9	8	25.01.2018	18
3	10.06.2017	10	9	13.04.2018	20
4	11.07.2017	11	10	08.06.2018	22
5	08.08.2017	12	11	16.07.2018	23
6	01.10.2017	14	12	04.08.2018	24

In campaigns 1 to 5 and 12, the starting and the ending benchmark of the profiles were connected to each other with precise levelling measurements (Tiryakioğlu *et al*., 2019). Thus, a spatial deformation amount for the years 2016 to 2018 was calculated for the other campaigns, and the movements in surface deformations were determined by measuring only along the profile. The height differences obtained by round-trip precise levelling in all benchmarks were calculated and used in the adjustment stage. Least Square Estimation (LSE) was used in the network adjustment. The network was initially free-adjusted, and Pope's Tau test was performed for outlier detection. A typical Conventional Deformation Analysis (CDA) method compares height differences in a levelling network between two different observation epochs. Since the height differences between the first benchmark of profiles 1 and 2 did not change in the link levelling between campaigns 1 to 5 and 12, the first benchmark of the first profile was assumed to be constant and the heights of all benchmarks are calculated by the methods specified in Tiryakioğlu *et al*. (2019). The obtained height differences are given in Fig. 5.

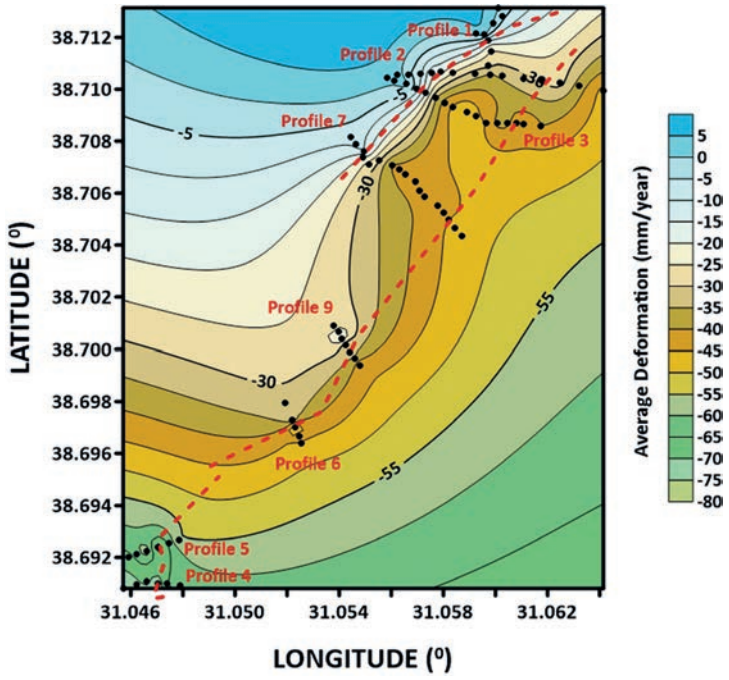

Fig. 5 - Vertical deformation map obtained from levelling.

The vertical deformations of the benchmarks reached -40 mm in the NE direction and -150 mm in the SW one. Similarly, a comparison of the amount of deformation of the benchmarks undertaken in relative terms showed that it increased from NW to SE. Similar results were obtained in other studies (Tiryakioglu *et al*., 2019; İmamoğlu *et al*., 2019). To provide a better understanding of the deformation behaviour of the region, eight profiles across the surface deformation lines were plotted (Figs. 6 to 11).

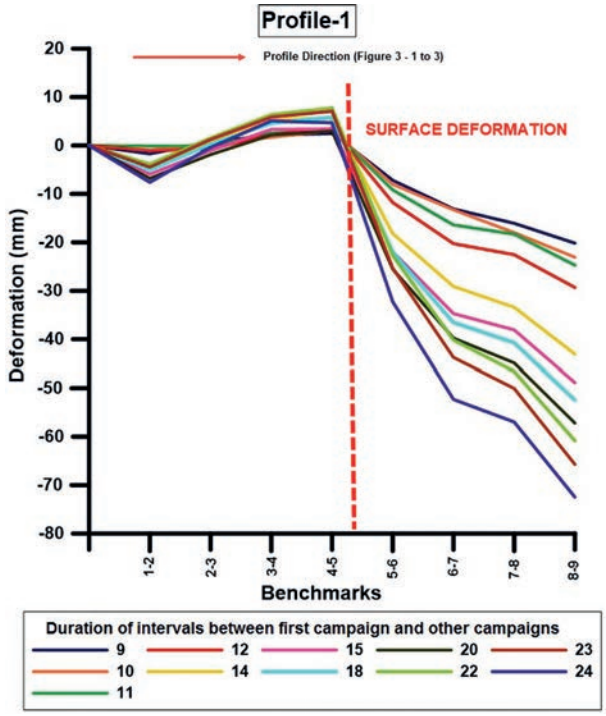

Fig. 6 - First profile deformations.

An examination of Fig. 6 shows that deformations starting from benchmark number 5 are observed in the first profile. It is clearly seen that those deformations increased with each day. While the amount of deformation was -29 mm at the end of the 12th month, it was -72 mm at the end of the 24th month.

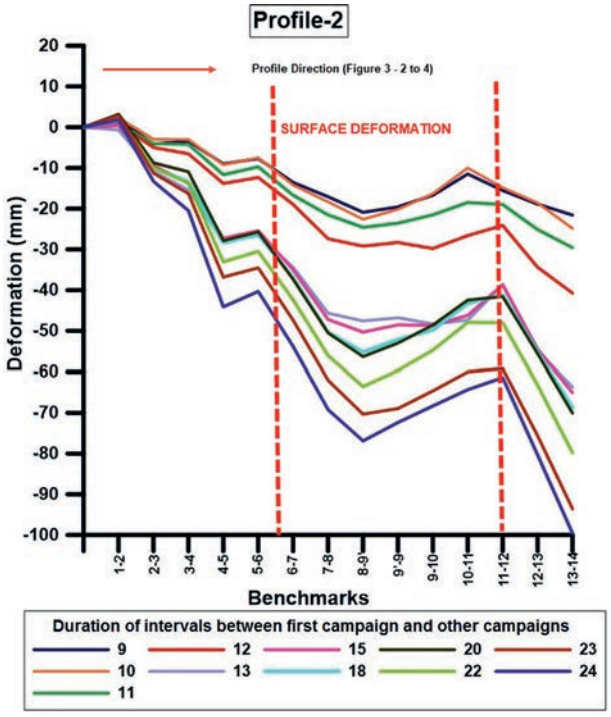

Fig. 7 - Second profile deformations.

Fig. 7 shows that deformations starting from benchmark number 2 can be seen in the second profile, and these deformations are increasing daily and continue after the ninth benchmark. In the same profile, declines are again seen subsequent to the 12th benchmark. The main reason for this situation was considered to be due to the second profile cutting into two surface deformations (Fig. 8). Similar results can also be found in profiles 3 and 7.

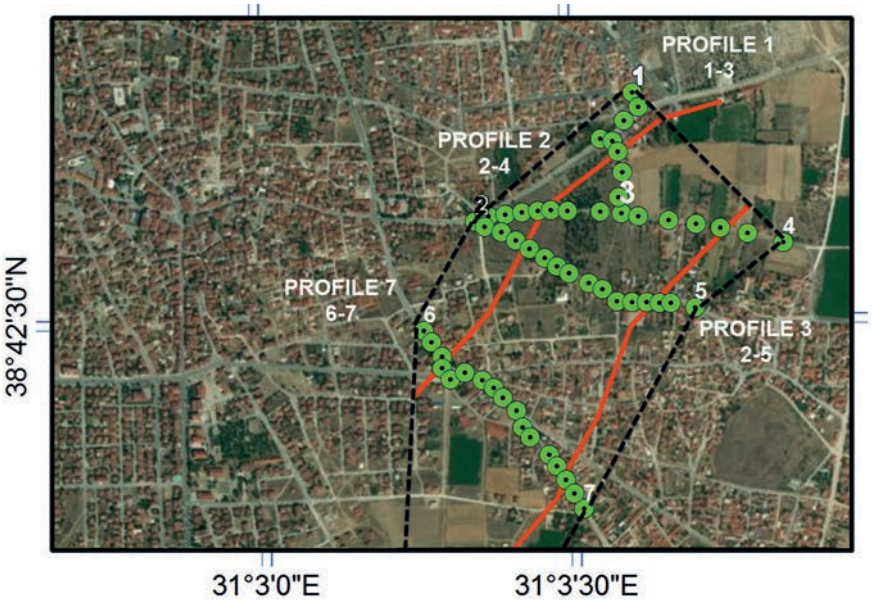

Fig. 8 - Profile cutting into two surface deformations.

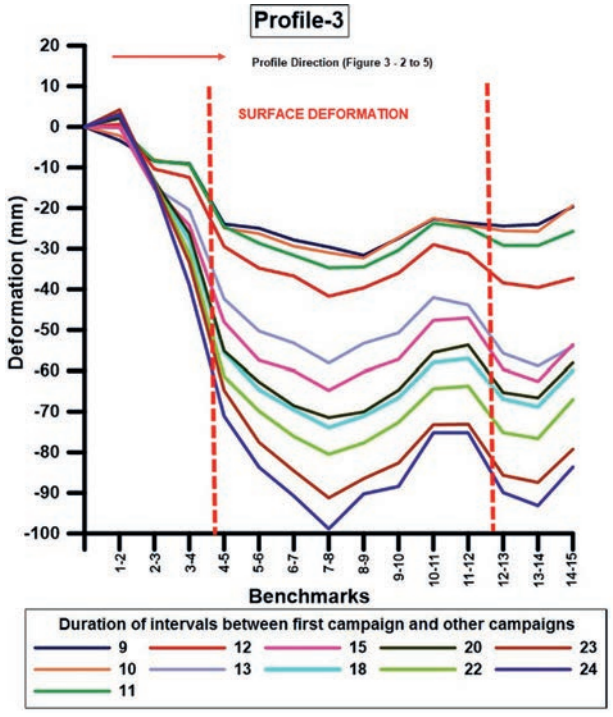

Fig. 9 - Third profile deformations.

Fig. 9 shows that while the amount of the deformation was -40 mm at the end of the 12th month, it was -99 mm at the end of the 24th month. Similar results were also found in profiles 6 to 9. Deformations were also observed from benchmark number 2 in the third profile (Fig. 10). When the amount of deformation was -37 mm at the end of the first year, it was -98 mm at the end of the second year.

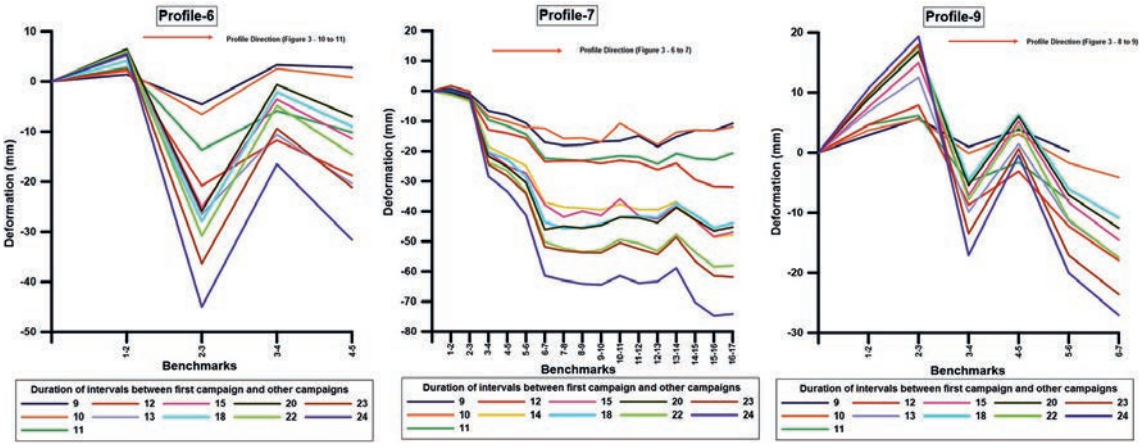

Fig. 10 - Sixth, seventh, and ninth profile deformations.

Deformation was observed from benchmark number 2 in the sixth profile. The amount of the deformation was -18 mm at the end of the first year and -31 mm at the end of the second year. The deformation was seen as starting from benchmark number 3 in the seventh profile. It was determined that the deformation was -31 mm at the end of the first year and -74 mm at the end of the second year. The deformations observed from benchmark number 3 in the eighth profile revealed that the amount of the deformation was -34 mm at the end of the first year and -81 mm at the end of the second year. In benchmark number 3 in the ninth profile, the deformation was observed to be -18 mm at the end of the first year and -27 mm at the end of the second year.

All figures indicate that all profiles contain every size of deformations, and seasonal deformation was increasing, especially in the summer months (12th and 24th months). Therefore, it was thought that deformation might be associated with underground water since it is well known that underground water levels decrease because of the intensive agricultural irrigation in the summer months in the region.

The Bolvadin settlement is located in the Akarçay basin, and in order to find the connection between the surface deformations and underground water, the data from three underground water wells (20953, 62421, 28372) in the region obtained from the 18th Regional Directorate of the State Hydraulic Works were evaluated. 20953 is one of the two wells closest to surface deformations, but the data of this well was not obtained after 2015 due to surface deformations, and well 62421 is far from the study area. Thus, only the data from the Bolvadin Centre well (28372) between 2008 and 2018 were used in the study. The data from this well between August 2016 and August 2018 were associated with the height differences obtained from the levelling studies (Fig. 12).

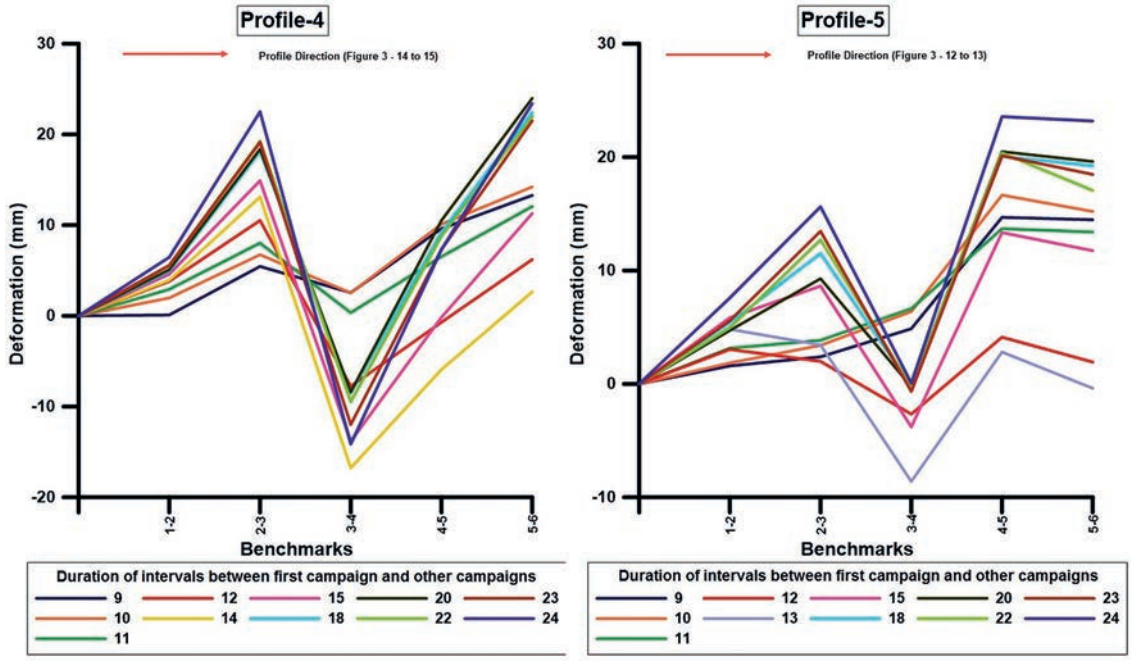

Fig. 11 - Fourth and fifth profile deformations.

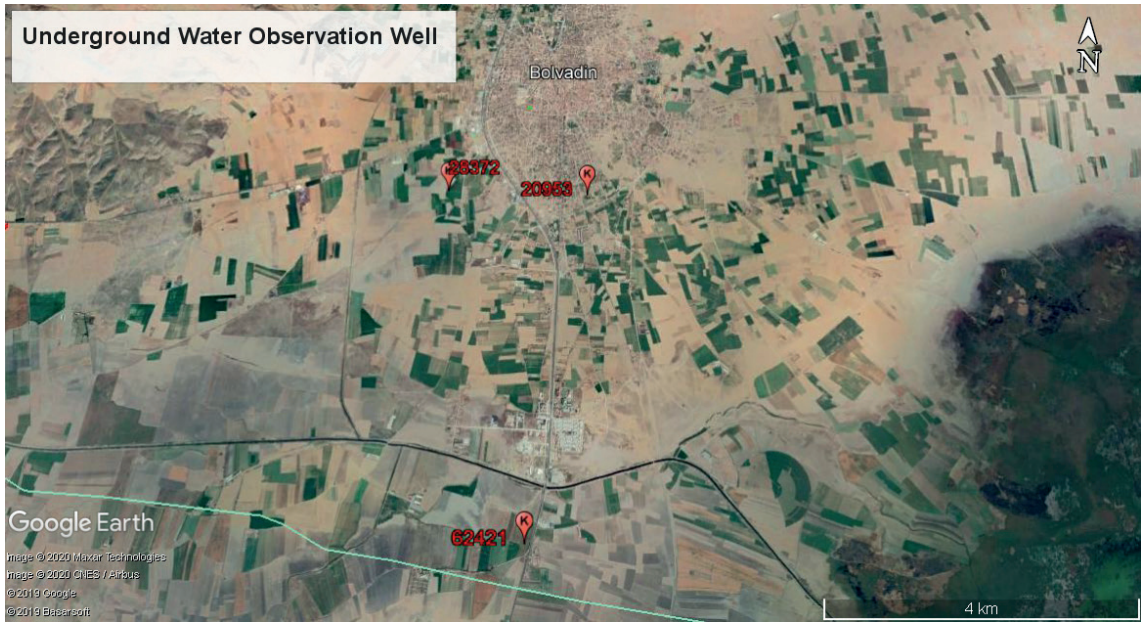

Fig. 12 - Underground water observation wells in the Bolvadin region.

It was observed that the water level of well 28372 had decreased from -16.5 to -26.5 m between August 2009 and August 2018. Seasonal fluctuations in the water levels occurred, and the water level, which decreased, especially in the summer months, increased in the months of November

and December. It was thought that the main reason for these changes was the presence of intensive agricultural irrigation in the region. Since the levelling studies started in August 2016, the current well values in the observation wells were also taken at that time (Fig. 13).

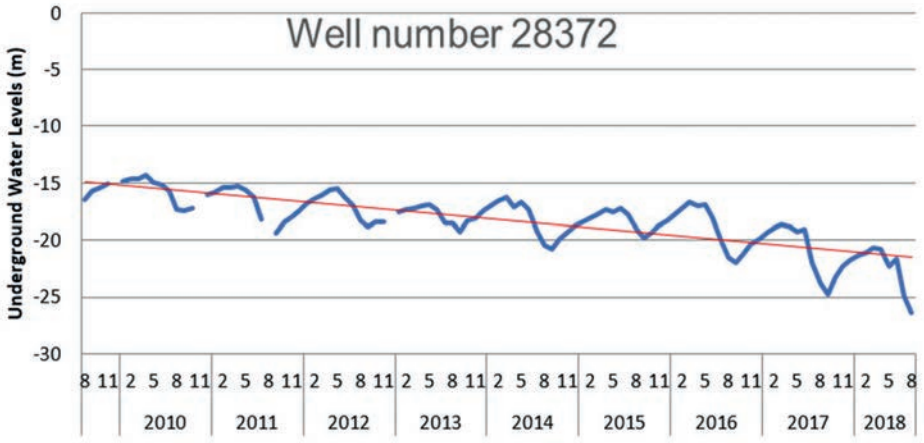

Fig. 13 - Underground water observation of the well 28372 in the centre of Bolvadin.

3. Relationship between levelling results and underground water levels

The most commonly used techniques for investigating the relationship between two quantitative variables are correlation and linear regression. Correlation quantifies the strength of the linear relationship between a pair of variables, whereas regression expresses the relationship in the form of an equation (Bewic *et al*., 2003). The relationship between the variables is calculated using the correlation coefficient. Multiple correlation criteria are used to determine which correlation coefficient to use. Simple correlation is a measure that determines the strength and direction of the relationship between two variables, *X* and *Y*. A simple correlation coefficient can range from -1 to 1. However, the maximum (or minimum) values of some simple correlations cannot achieve unity (i.e. 1 or -1). There is more than one correlation coefficient calculating method with the Pearson, Spearman-Rank, and Kendall-Tau correlation coefficients being the most widely used (Bewick *et al*., 2003). Pearson-Moment correlation coefficient is calculated using the following equations in a linear data group of two variables with *N* observations.

$$r_{xy} = \frac{\sum_{i=1}^{n}(X_i - \bar{X})(Y_i - \bar{Y})}{\sqrt{\sum_{i=1}^{n}(X_i - \bar{X})^2 \sum_{i=1}^{n}(Y - \bar{Y})^2}} \quad (1)$$

$$r_{xy} = \frac{\sum d_x d_y}{\sqrt{\left(\sum d_x^2\right)\left(\sum d_y^2\right)}} \quad (2)$$

In the equations given above, $\sum d_x d_y$ is the sum of products, $\sum d_x^2$ and $\sum d_y^2$ are the sums

of squares associated with X and Y, respectively. In order to determine whether the correlation coefficient found by this method is statistically significant, the hypothesis $H_0: \rho_{xy} = 0$ is tested.

$H_1: \rho_{xy} \neq 0$ is assumed. The test statistics required to test the H_0 hypothesis is calculated as follows:

$$t = \frac{r_{xy}}{\sqrt{\frac{1 - r_{xy}^2}{n-2}}} . \tag{3}$$

If the calculated t-value is equal to, or greater than, the value in the t-table with n-2 degree of freedom, the hypothesis H_0 is rejected. Otherwise, it is accepted.

The Spearman-Rank correlation coefficient is calculated with the ranks. $R(x)$ and $R(y)$ are the Spearman-Rank correlation coefficients calculated in Eq. 4 to show the rank of the variable pairs of (X_i, Y_i):

$$r_s = \frac{\sum_{i=1}^{n} R(x_i)R(y_i) - n\left(\frac{n+1}{2}\right)^2}{\sqrt{\left(\sum_{i=1}^{n} R(x_i)^2 - n\left(\frac{n+1}{2}\right)^2\right)\left(\sum_{i=1}^{n} R(y_i)^2 - n\left(\frac{n+1}{2}\right)^2\right)}} . \tag{4}$$

If there are no values with the same ranks among the observations, the Spearman-Rank correlation coefficient for two variables, such as X and Y, is calculated as in the Pearson correlation coefficient in Eq. 1. If the data sets have the same rank values, then the Spearman-Rank correlation coefficient, $d(i) = X_i - Y_i$ $i = 1, 2, \ldots, n$ is calculated with the following equation:

$$r_s = \frac{6\sum_{i=1}^{n} d_i^2}{n\left(n^2 - 1\right)} . \tag{5}$$

When the Spearman-Rank correlation coefficient calculated to test the hypothesis of $H_0: \rho_{xy} = 0$ is greater than, or equal to, the table value specially prepared for this purpose, the H_0 hypothesis is rejected. Kendall-Tau correlation coefficient between variable pairs of (X_i, Y_i) is calculated by the following equation:

$$\frac{\textit{Number of matching observation pair} - \textit{Number of mismatching observation pair}}{\frac{1}{2}n(n-1)} \tag{6}$$

If the observation pairs of (X_i, Y_i) and (X_j, Y_j) meet the requirements of $X_i > X_j$ and $Y_i > Y_j$ or $X_i < X_j$ and $Y_i < Y_j$, it is called the matching observation pair. If they do not, such as $X_i > X_j$ and $Y_i < Y_j$ or $X_i < X_j$ and $Y_i > Y_j$, they are referred to as mismatching observation pair.

The Z-test statistic that is required to test the $H_0: \rho_{xy} = 0$ hypothesis is calculated by the following equation:

$$Z = \frac{3_T\sqrt{n(n-1)}}{\sqrt{2(2n+5)}} . \tag{7}$$

If $Z \geq 1.96$, the hypothesis H_0 is rejected. Otherwise, the H_0 hypothesis is accepted.

The following comments can be made about the obtained *r*-value:
0.00: no relationship;
0.01 - 0.29: low-level relationship;
0.30 - 0.70: moderate relationship;
0.71 - 0.99: high-level relationship;
1.00: can be interpreted as the perfect relationship.

The relationship between the surface deformations occurring in the region and the underground water levels was investigated based on two years of data from underground water observations at well number 28372. For this purpose, the relationship between the results of the levelling deformation measurements conducted between 2016 and 2018 and fluctuations in the underground water levels was examined. In the comparison, revealing the relationship between these two variables was attempted by calculating the correlation coefficient of the Pearson, Spearman-Rank, and Kendall-Tau.

In this study, the long duration changes of the observation of well number 28372 belonging to the State Hydraulic Works in the Bolvadin settlement and the correlation between the surface deformations occurring in the region were analysed by calculating the correlation coefficients of Pearson, Spearman-Rank, and Kendall-Tau.

In total, three correlation functions were utilised. The correlation coefficients of Kendal, Spearman, and Pearson were obtained for every profile, their significance values were calculated, and this information is given in Table 2. If one of the three correlation coefficients calculated for every profile was meaningful or significant, the existence of a correlation among the data was accepted. If the *P*-coefficient (probability value) was between 0 and 0.5, there was significance or meaningfulness with at least a 95% probability (Bewick *et al*., 2003). Moreover, with regard to the size of the correlation coefficient, information about the power of the correlation were acquired. When Table 2 is examined, it can be seen that there is no relationship between the underground water and the deformation for the fourth and fifth profiles. At least one of the correlation methods applied to all other profiles was significant or meaningful.

4. Results and conclusions

Aseismic surface deformations which have been occurred after the 2003 Çay earthquakes (*M* 6.3 and 6.0) were observed in the Bolvadin settlement.

According to the recent studies the surface linear deformations are developed on the Bolvadin Fault which is an NE-SW trending active normal fault and could generate destructive earthquakes up to magnitude 6.5 (Özkaymak *et al*., 2017, 2019). Along the 4-km long linear deformation zone consisting of three splays, the total vertical displacement is about 50 cm (Özkaymak *et al*., 2017). Eight levelling profiles were established in the region in order to investigate the sizes of these surface deformations. Those profiles were constituted perpendicular to the surface deformations in a profile shape. The levelling measurements, composed of 12 campaigns, were undertaken in the period from 2016 to 2018. All the levelling measurements were completed using the invar barcoded levelling rods based on the BFFB method. Furthermore, the underground water level of well 28372, located in the county town, was provided by the 18th Regional Directorate of the State Hydraulic Works. The relationship between the levelling measurements and the underground

Table 2 - Coefficient of correlation.

1. Profile Correlation Compatibility Test Result			
Correlation methods	Coefficient of correlation	*P*-Value	Decision
Kendall Rank	0. 0.0672	0.3517	Meaningfulness
Spearman's Rank-Order	0.0911	0.3776	Meaningfulness
Pearson Product-Moment	0.2071	0.0429	Significant
2. Profile Correlation Compatibility Test Result			
Correlation methods	Coefficient of correlation	*P*-Value	Decision
Kendall Rank	0.2501	0.0000	Significant
Spearman's Rank-Order	0.3543	0.0000	Significant
Pearson Product-Moment	0.4240	0.0000	Significant
3. Profile Correlation Compatibility Test Result			
Correlation methods	Coefficient of correlation	*P*-Value	Decision
Kendall Rank	0.2470	0.0000	Significant
Spearman's Rank-Order	0.3594	0.0000	Significant
Pearson Product-Moment	0.4096	0.0000	Significant
4. Profile Correlation Compatibility Test Result			
Correlation methods	Coefficient of correlation	*P*-Value	Decision
Kendall Rank	0.0335	0.7198	Meaningfulness
Spearman's Rank-Order	0.0358	0.7858	Meaningfulness
Pearson Product-Moment	0.0194	0.8830	Meaningfulness
5. Profile Correlation Compatibility Test Result			
Correlation methods	Coefficient of correlation	*P*-Value	Decision
Kendall Rank	0.0246	0.7928	Meaningfulness
Spearman's Rank-Order	0.0195	0.8823	Meaningfulness
Pearson Product-Moment	0.0586	0.6566	Meaningfulness
6. Profile Correlation Compatibility Test Result			
Correlation methods	Coefficient of correlation	*P*-Value	Decision
Kendall Rank	0.2866	0.0055	Significant
Spearman's Rank-Order	0.3782	0.0080	Significant
Pearson Product-Moment	0.4571	0.0011	Significant
7. Profile Correlation Compatibility Test Result			
Correlation methods	Coefficient of correlation	*P*-Value	Decision
Kendall Rank	0.2859	0.0000	Significant
Spearman's Rank-Order	0.3999	0.0000	Significant
Pearson Product-Moment	0.4527	0.0000	Significant
9. Profile Correlation Compatibility Test Result			
Correlation methods	Coefficient of correlation	*P*-Value	Decision
Kendall Rank	0.1437	0.0857	Meaningfulness
Spearman's Rank-Order	0.1920	0.1061	Meaningfulness
Pearson Product-Moment	0.2329	0.0490	Significant

water levels, on the date when the measurement was made, was analysed and the obtained data revealed the following results.

The vertical deformations occurring on the surface have been increasing over time (Figs. 6 to 11). The deformation amounts varied between a total of 40 and 100 mm in two years. The first profile is located in the most north-western point of the surface deformation line. This profile cuts only one surface deformation, and a deformation of -72 mm was found between the first and the last campaign. It was observed that while this deformation was -29 mm between August 2016 and August 2017, it reached -43 mm between August 2017 and August 2018 (Fig. 6). Additionally, the second, third, and seventh profiles cut two surface ruptures (Figs. 7, 8, and 10). The deformation amounts in those profiles reached -100, -100, and -75 mm, respectively, at the end of the second year. Due to the two surface ruptures, more deformation occurred in these three profiles than in the first one. While those deformations in the second and third profiles were approximately -40 mm in the first year, they increased to -60 mm in the second year. It is seen that the deformations increased about 10 mm in the south-western part of the region for each rupture.

It was observed that the deformation was -18 mm in the first year and reached 31 mm at the end of the second year in the sixth profile, -31 mm in the first year, reaching -74 mm at the end of the second year for the seventh profile, -34 mm in the first year, reaching -81 mm at the end of the second year for the eighth profile, and finally -18 mm in the first year, reaching -27 mm at the end of the second year for the ninth profile. A fair amount of increase in the profiles and the decrease in the deformation amount was seen in the profiles two, three, and seven after two ruptures.

When the deformations graphics are examined, it can be seen that deformation increases, especially in the summer months (12th and 24th months). Based on this increase in those months, it was considered that the deformation might be related to the underground water. When the well records were analysed, it was observed that the level of underground water had decreased by approximately 3-5 m in two years. Therefore, the correlation between the data on underground water levels taken from State Hydraulic Works and the deformation amounts was examined. The Kendal, Spearman, and Pearson correlation methods were used and are presented in Table 2. If one of the three correlation coefficients calculated for every profile was significant or meaningful, a correlation among the data was assumed to exist. According to these results, it can be seen that there is no relation between underground waters and deformation for the fourth and fifth profiles.

In addition to the above examination, when the calculated correlation coefficients were scrutinised there was low-level significance in the first and ninth profiles and a moderate relationship significance in the second, third, sixth, seventh, and eight profiles. A non-existence of relationships in the fourth and fifth profiles was discovered with the correlation and calculated *P*-coefficient. Consequently, it was seen that there was a statistically moderate relationship between underground water levels and deformations. The correlation levels calculated on all routes, being medium, indicate that the surface deformations not only result from the groundwater level change, but are also of a tectonic origin.

Some recent studies conducted on surface deformations on active fault in the Sarigöl region proved that tectonism plays a role in the aseismic surface deformations in western Anatolia (Koca *et al*., 2011). Beside this, some studies suggest that similar situation may occur in the Bolvadin settlement area (Özkaymak *et al*., 2017, 2019; Tiryakioğlu *et al*., 2019). The approximately 3.5 m decline in the underground water level within the last two years in the Bolvadin area and the corresponding consolidation of the ground make a great contribution to the formation of ruptures.

However, according to the paleoseismological studies on the BF, at least two earthquakes occurred in the historical period (the first one in 530 and the other in 1549) (Özkaymak *et al*., 2019). In addition, due to the existence of earthquakes generating surface rupture in the region in recent years, it is evidenced that the BF is an active fault. So, the deformations on this active fault are probably related with the post seismic behaviour of the 2003 Çay earthquakes and tectonic loading on the northern border fault of AAG.

However, permanent GNSS stations have to be established in order to monitor the deformations. In particular, the origin of deformations should be investigated by multidisciplinary geologic and geodetic studies (seismicity, drilling, geotechnic, seismic reflection studies, LIDAR).

Acknowledgements. This research was supported by the TUBITAK (project number: 115Y246). We thank the Turkish State Hydraulic Works for providing groundwater level data. M.A. Dereli is acknowledged for the statistical evaluation. H.B. Bozkuş carried out the fieldwork as part of his M.Sc. dissertation.

REFERENCES

Amighpey M. and Arabi S.; 2016: *Studying land subsidence in Yazd province, Iran, by integration of InSAR and levelling measurements*. Remote Sens. Appl.: Soc. Environ., **4,** 1-8.

Bewick V., Cheek L. and Ball J.; 2003: *Statistics review 7: correlation and regression*. Crit. Care**, 7,** 451, doi: 10.1186/cc2401.

Blumenthal M.; 1963: *Le systeme structural du Taurus sud-Anatolien*. Mem. Soc. Geol. Fr., **2,** 611-662.

D'Anastasio E., De Martini P.M., Selvaggi G., Pantosti D., Marchioni A. and Maseroli R.; 2006: *Short-term vertical velocity field in the Apennines (Italy) revealed by geodetic levelling data*. Tectonophys., **418,** 219-234.

Emre Ö., Duman T.Y., Özalp S., Olgun Ş. and Elmaci H.; 2011: *1: 250.000 scale active fault map series of Turkey, Afyon (NJ 36-5) quadrangle*. General Directorate of Mineral Research and Exploration, General Directorate of Mineral Research and Expansion Direction (MTA), Ankara, Turkey, n. 16.

Hao M., Wang Q., Shen Z., Cui D., Ji L., Li Y. and Qin S.; 2014: *Present day crustal vertical movement inferred from precise levelling data in eastern margin of Tibetan Plateau*. Tectonophys., **632,** 281-292.

Holzer T.L.; 1980: *Faulting caused by ground-water level declines, San Joaquin Valley, California*. Water Resour. Res., **16**, 1065-1070.

Holzer T.L.; 1984: *Ground failure induced by groundwater withdrawal from unconsolidated sediment*. In: Holzer T.L. (ed), Man-induced land subsidence, Geological Society of America, CO, USA, vol. 6, pp. 67-105, doi: 10.1130/REG6-p67.

Holzer T.L. and Galloway D.L.; 2005: *Impacts of land subsidence caused by withdrawal of underground fluids in the United States*. In: Ehlen J., Haneberg W.C. and Larson R.A. (eds), Humans as geologic agents, Geological Society of America, CO, USA, vol. 16, pp. 87-99, doi: 10.1130/2005.4016(08).

Imamoglu M., Kahraman F., Cakir Z. and Sanli F.B.; 2019: *Ground deformation analysis of Bolvadin (W. Turkey) by means of multi-temporal InSAR techniques and Sentinel-1 data*. Remote Sens., **11**, 1069; doi: 10.3390/rs11091069.

Kall T., Oja T. and Tänavsuu K.; 2014: *Postglacial land uplift in Estonia based on four precise levellings*. Tectonophys., **610**, 25-38, doi: 10.1016/j.tecto.2013.10.002.

Kaymakci N.; 2006: *Kinematic development and paleostress analysis of the Denizli basin (western Turkey): implications of spatial variation of relative paleostress magnitudes and orientations*. J. Asian Earth Sci., **27,** 207-222.

Koca M.Y., Sözbilir H. and Uzel, B.; 2011: *Sarıgöl Fay Zonu Boyunca Meydana Gelen Deformasyonların Nedenleri Üzerine bir araştırma*. Jeoloji Mühendisliği Dergisi, **35**, 151-173 (in Turkish).

Koçyiğit A.; 1984: *Güneybatı Türkiye ve yakın dolayında levha içi yeni tektonik gelişim*. Türkiye Jeoloji Kurumu Bülteni, **27**, 1- 15 (in Turkish).

Koçyiğit A. and Özacar A.; 2003: *Extensional neotectonic regime through the NE edge of outer Isparta Angle, SW Turkey: new field and seismic data*. Turk. J. Earth Sci., **12,** 67-90.

Koçyiğit A., Ünay E. and Saraç G.; 2000: *Episodic graben formation and extensional neotectonic regime in west central Anatolia and the Isparta Angle: a case study in the Akşehir - Afyon Graben, Turkey*. Geol. Soc. London, Spec. Publ., **173,** 405-421, doi: 10.1144/GSL.SP.2000.173.01.19.

Murasea M., Matta N., Lin C.H., Chen W.S. and Koizumie N.; 2013: *An episodic creep slip event detected by a precise levelling surveys at the central part of the Longitudinal Valley Fault, eastern Taiwan*. Tectonophys., **608,** 904-913.

Özkaymak Ç.; 2015: *Tectonic analysis of the Honaz fault (western Anatolia) using geomorphic indices and the regional implications*. Geodinamica Acta, **27**, 110-129.

Özkaymak Ç, Sözbilir H., Tiryakioğlu İ. and Baybura T.; 2017: *Geologic, geomorphologic and geodetic analyses of surface deformations observed in Bolvadin (Afyon - Akşehir Graben, Afyon)*. Geol. Bull. Turkey, **60,** 169-188.

Özkaymak Ç., Sözbilir H., Gecievi M. and Tiryakioğlu I.; 2019: *Late Holocene coseismic rupture and aseismic creep on the Bolvadin Fault, Afyon Akşehir Graben, western Anatolia*. Turk. J. Earth Sci., **28**, 787-804.

Pacheco-Martínez J., Hernández-Marin M., Burbey T.J., González-Cervantes N., Ortiz J., de Leon M.E.Z. and Solís-Pinto A.; 2013: *Land subsidence and ground failure associated to groundwater exploitation in the Aguascalientes Valley*, *México*. Eng. Geol., **164,** 172-186.

Péwé T.L.; 1990: *Land subsidence and earth-fissure formation caused by groundwater withdrawal in Arizona; a review*. In: Higgins C.G. and Coates D.R. (eds), Groundwater geomorphology; the role of subsurface water in Earth-surface processes and landforms, Special paper 252, Geological Society of America, Boulder Co., U.S.A., pp. 219-233.

Poyraz F., Hastaoğlu K.O., Koçbulut F., Tiryakioğlu I., Tatar O., Demirel M., Duman H., Aydin C., Ciğer A.F., Gursoy O., Turk T. and Sigirci R.; 2019: *Determination of the block movements in the eastern section of the Gediz Graben (Turkey) from GNSS measurements*. J. Geodyn., **123**, 38-48, doi: 10.1016/j.jog.2018.11.001.

Qin S., Wang W. and Song S.; 2018: *Comparative study on vertical deformation based on GNSS and levelling data*. Geod. Geodyn., **9**, 115-120.

Rüeger J.M.; 2000: *The topcon DL-101C digital level*. Aust. Surv., **45,** 62-70.

Sabuncu A. and Ozener H.; 2014: *Monitoring vertical displacements by precise levelling: a case study along the Tuzla Fault, Izmir, Turkey*. Geomat. Nat. Haz. Risk, **5,** 320-333, doi: 10.1080/19475705.2013.810179.

Tiryakioğlu İ., Özkaymak Ç., Baybura T., Sözbilir H. and Uysal M.; 2018a: *Comparison of palaeostress analysis, geodetic strain rates and seismic data in the western part of the Sultandağı Fault in Turkey*. Ann. Geophys., **61**, GD335, doi: 10.4401/ag-7591.

Tiryakioğlu İ., Uğur M.A. and Özkaymak Ç.; 2018b: *Determination of surface deformations with global navigation satellite system time series*. Int. J. Geol. Environ. Eng., **12**, 719-722.

Tiryakioğlu İ., Yiğit C.O., Özkaymak Ç., Baybura T., Yilmaz M., Uğur M.A., Yalçın M.A., Poyraz F., Sözbilir H. and Gülal E.; 2019: *Active surface deformations detected by precise levelling surveys in the Afyon-Akşehir Graben, western Anatolia*, *Turkey*. Geofiz., **36,** 33-52, doi: 10.15233/gfz.2019.36.4.

Turan N.; 2002: *Geological map of Turkey in 1:500.000 scale: Ankara sheet*. Publication of Mineral Research and Explanation Direction of Turkey (MTA), Ankara, Turkey.

Corresponding author: İbrahim Tiryakioğlu
Department of Geomatics, Faculty of Engineering, Afyon Kocatepe University
ANS Campus, TR-03200, Afyonkarahisar, Turkey
Phone: +90 2722281423; fax: +90 2722281422; e-mail: itiryakioglu@aku.edu.tr